Pergamon

Bioorganic & Medicinal Chemistry 9 (2001) 3255–3264

BIOORGANIC & MEDICINAL CHEMISTRY

A Bicyclic and Hsst2 Selective Somatostatin Analogue: Design, Synthesis, Conformational Analysis and Binding

Eliezer Falb,[a] Yoseph Salitra,[a] Tamar Yechezkel,[a] Moshe Bracha,[a] Pninit Litman,[a] Roberto Olender,[a] Rakefet Rosenfeld,[a,†] Hanoch Senderowitz,[a] Shaokai Jiang[b] and Murray Goodman[b,*]

[a]*Peptor Ltd., Kiryat Weizmann 16, Rehovot 76326, Israel*
[b]*Department of Chemistry and Biochemistry, University of California at San Diego, La Jolla, CA 92093-0343, USA*

Received 7 May 2001; accepted 25 June 2001

Abstract—A backbone bridged and disulfide bridged bicyclic somatostatin analogue, compound **1** (PTR-3205), was designed and synthesized by solid-phase methodology. The binding of compound **1** to the five different somatostatin receptors, expressed in CHO or COS-7 cells, indicate a high degree of selectivity towards hsstr2. The three-dimensional structure of this compound has been determined in DMSO-d_6 and in water by ^{1}H NMR and by molecular dynamics simulations. Similar backbone conformations were observed in both solvents. We have established direct evidence that the backbone of this bicyclic somatostatin analogue assumes a 'folded' conformation in solution, where the lactam ring extends roughly in the plane of the β-turn. The pharmacophoric region Phe-(D)-Trp-Lys-Thr of compound **1** is in accord with that of both the Veber compound L-363,301 (Merck) and sandostatin. We believe that the enhanced selectivity towards the hsst2 receptor, in comparison with other analogues, is due to its large hydrophobic region, composed of the lactam ring and the Phe side chains at positions 1 and 8.

Introduction

Somatostatin is a cyclic tetradecapeptide hormone that was isolated for the first time in 1973 as an inhibitor of growth hormone release.[1] Somatostatin has a major regulatory effect. It inhibits the release of numerous hormones such as insulin, glucagon, gastrin, secretin and growth hormone.[2] In the central nervous system, somatostatin acts as a neurotransmitter and neuromodulator.[3] It also has antiproliferative effects, regulating cell proliferation and differentiation.[4]

The diverse biological activities of somatostatin are mediated by a family of five cell surface receptors, hsst1-5. Due to its broad spectrum of physiological activities, somatostatin has been, and continues to be, a target for extensive studies for the development of small receptor subtype specific analogues.

Veber et al.[5a] at Merck synthesized cyclic hexapeptide analogues of somatostatin and demonstrated that the central tetrapeptide Phe^7-(D)-Trp^8-Lys^9-Thr^{10} (the numbering follows that of the native somatostatin-14, H-Ala^1-Gly^2-c[Cys^3-Lys^4-Asn^5-Phe^6-Phe^7-Trp^8-Lys^9-Thr^{10}-Phe^{11}-Thr^{12}-Ser^{13}-Cys^{14}]-OH) contains the somatostatin pharmacophore. The Merck group has also shown that the lysine and D-tryptophan side chains in these cyclic hexapeptides exist in an equatorial orientation relative to the backbone of the peptides.[5b,c] This conclusion was obtained from NMR data, based on an upfield shift of the lysine γ-methylene of about 1 ppm and a 'correlation of the shift with the conformation at biological receptors'.[5b] Since then, numerous hexa- and octapeptide analogues of somatostatin have been synthesized and characterized either through receptor binding or functional bioassays.[6] Among these, sandostatin[7] is a potent inhibitor of growth hormone secretion and is in clinical use for the treatment of several endocrine and malignant disorders. Sandostatin, (D)-Phe-c[Cys-Phe-(D)-Trp-Lys-Thr-Cys]-Thr-ol binds predominantly to hsstr2 and hsstr5 and with low affinity to hsstr3. Sandostatin has been the subject of extensive structural studies, including NMR[8] and X-ray diffraction.[9] Taken together these studies have demonstrated that sandostatin

*Corresponding author. Fax: +1-858-534-0202; e-mail: mgoodman@ucsd.edu
†Current address: QBI Enterprises Ltd., Weizmann Science Park, PO Box 4071, Ness Ziona 70400, Israel.

0968-0896/01/$ - see front matter
PII: S0968-0896(01)00234-6

in solution exists in two conformational families, differing mainly by the conformation of the C-terminal tail. The molecule adopts an overall antiparallel β-sheet conformation, with a type II′ β-turn centered at the (D)-Trp[8]-Lys[9] region. In one conformational family, the residues following this β-turn continue the β-sheet structure. Based on elaborate SAR studies of various somatostatin analogues, Goodman et al.[8] concluded that this family contains the active conformation(s). In the second conformational family, the residues following the β-turn adopt a 3_{10} helical conformation.

In this paper we describe the design, synthesis, bioactivity and conformational analysis of compound **1** (Fig. 1), a bicyclic analogue of somatostatin in which the two tail fragments of sandostatin are cyclized via backbone cyclization.[10] The backbone bridge was designed in an attempt to preserve the bioactive conformation of sandostatin by constraining the N- and C-termini while stabilizing the type II′ β-turn region of the molecule. The resulting analogue is a highly selective hsst2 binding sandostatin mimetic.

Results and Discussion

Design

Our aim was to design a bicyclic sandostatin-like analogue of somatostatin, constrained in the proposed bioactive conformation. Backbone cyclization is an appropriate synthetic strategy to achieve this goal because it allows the bridging of any two backbone nitrogens to create cyclic structures of various sizes. We describe analyses of a bicyclic structure of a sandostatin analogue where the bridge lies between positions 1 and 8. In order to utilize this approach, we created a virtual database of backbone bridges, NH_2–$(CH_2)_n$–NH-C(O)–$(CH_2)_m$–NH_2, where $n = 2$-4, $m = 1$–5, and $n + m \leq 7$ and the two terminal amino groups represent the backbone nitrogens of the peptide. The database was created by performing a systematic conformational search on all rotatable bonds within each bridge (at 20 degree intervals). The search was performed using the Search/Compare module of INSIGHT.[11] The final database contains an order of 10^4 entries. Starting with the proposed bioactive conformation of sandostatin, we then searched the database for bridges that connect the two tails of this molecule without any conformational distortion. To this end, four geometrical parameters were defined for the sandostatin backbone, namely the **N**(Phe[1])...**N**(Thr[8]) distance, the **H**–**N**(Phe[1])...**N**(Thr[8]) and **N**(Phe[1])...**N**–**H**(Thr[8]) angles and the **H**–**N**(Phe[1])...**N**–**H**(Thr[8]) torsion. These parameters were compared with their respective counterparts in the virtual library of backbone bridges (N–N distance, C–N...N and N...N–C angles and C–N...N–C torsion) and only those bridges matching all four parameters for sandostatin, within a pre-determined tolerance, were considered. The selected bridges were attached to the corresponding positions on the backbone and further optimized, maintaining the rigidity of the backbone. This procedure identified several potential bridges and the choice for synthesis was made based on the energy ranking of each potential bridge. We selected and incorporated the bridge structure NH_2–$(CH_2)_3$–C(O)–NH–$CH_2)_3$–NH_2 into our bicyclic sandostatin design. In addition, we replaced Thr[8] with Phe since several sandostatin-like analogues, in which Phe substitutes Thr[8], show biological activities similar to that of sandostatin.[12] Figure 1 shows the chemical structure of the bicyclic sandostatin analogue compound **1** (PTR-3205).

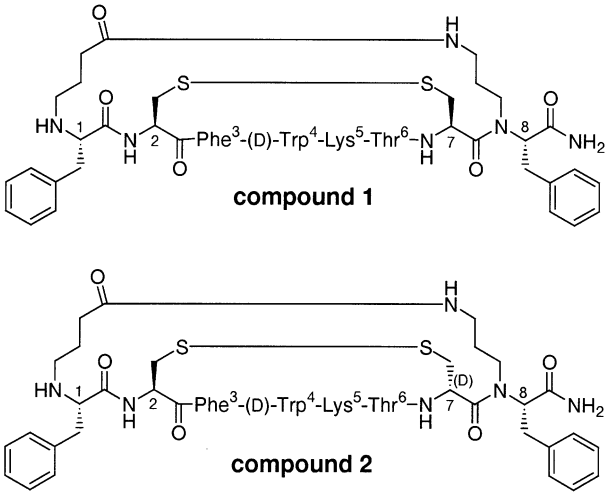

Figure 1. Structure of bicyclic somatostatin analogue **1** and its (D)-Cys[7] epimer **2**.

Synthesis

The synthesis of compound 1 (PTR-3205) was carried out on the solid phase using Fmoc protection and PyBroP coupling (Scheme 1). Derivatized Phe residues were incorporated into the peptide sequence with *N*-aminopropyl Phe (PheN3) in position 8 and *N*-carboxypropyl Phe (PheC3) in position 1. The coupling of Fmoc-Cys(Acm)-OH to the sterically hindered secondary amine of the PheN3-peptidyl-resin at position 8 was done using bis(trichloromethyl) carbonate (BTC).[13] The carboxy and amino groups of the *N*-alkylated Phe residues were protected as their allyl and allyloxycarbonyl (Alloc) derivatives, respectively. Upon removal of the allyl and Alloc protecting groups by $Pd(PPh_3)_4$, the linear peptide was cyclized using PyBOP to form the backbone bridge. A second intramolecular cyclization via oxidation[14] of the S(Acm) groups by I_2 formed the disulfide bridge. Cleavage with TFA followed by precipitation with diethyl ether afforded the crude bicyclic peptide 1.

The HPLC profile of the crude peptide presented two peaks in a 1:5 ratio (Fig. 2). These two peaks were separated and isolated by preparative reverse-phase HPLC. Mass spectrometry indicated the molecular weights of the two compounds to be identical and in agreement with the expected mass of the bicyclic peptide. Optical purity analysis of the amino acids of each peptide (carried out at C.A.T. GmbH, Germany) indicated a high level of epimerization at Cys[7] in the minor

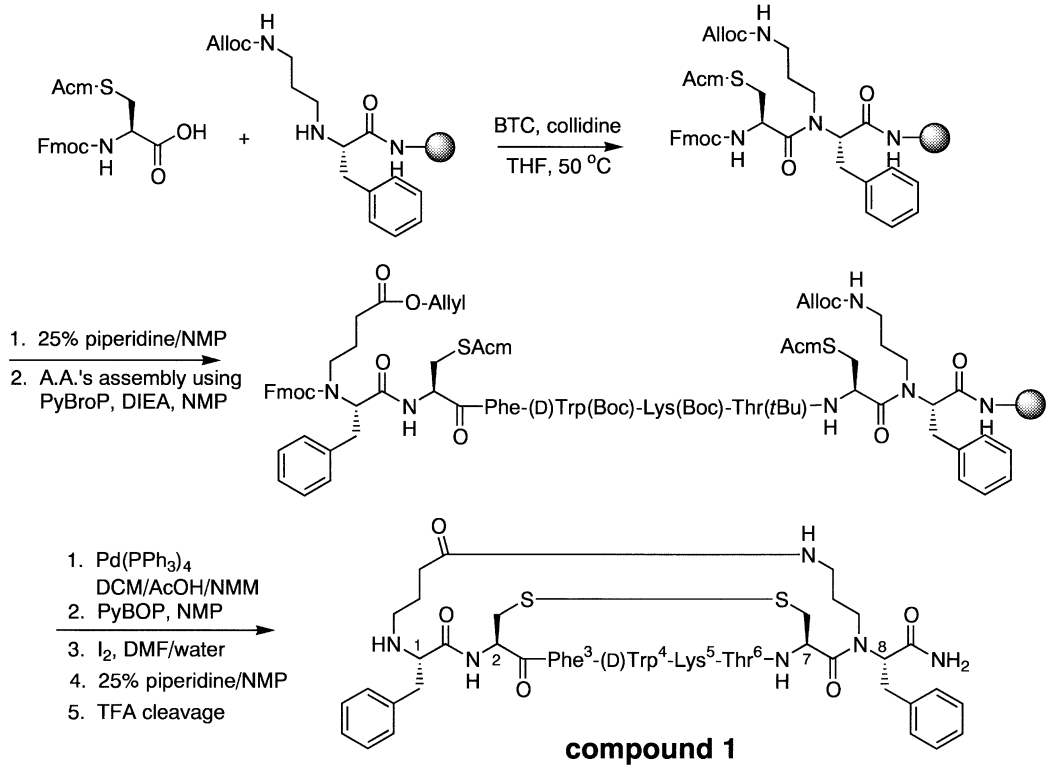

Scheme 1.

component with a (D/L)/Cys ratio of ~1:1 (Table 1). Apparently, the BTC coupling of Fmoc-Cys(Acm)-OH to the sterically hindered PheN3-peptidyl resin resulted in partial racemization to form both the desired peptide 1 and its Cys^7 epimer 2 (Fig. 1). In short, the optical purity analysis was carried out at C.A.T. GmbH as follows: the peptide was hydrolyzed with 6 N HCl at 110 °C for 24 h, and the mixture was injected into a gas chromatograph.

Receptor binding assays

The ability of compound **1** to inhibit binding of radiolabeled somatostatin was determined using membranes prepared from CHO-K1 cells (in the case of receptor subtypes 1, 2, 3 and 5) or COS-7 cells (in the case of receptor subtype 4) which are stable for expressing individually cloned somatostatin receptors. The results demonstrate a high degree of selectivity towards hsst2 with an IC_{50} of 3.7 nM (Fig. 3). The IC_{50} values for binding to the other receptors are at least two orders of magnitude lower.

NMR analysis

Backbone conformation. In an attempt to clarify the observed selectivity of compound **1** towards hsstr2, we have determined its 3-D structure in water and in DMSO-d_6 by ^{1}H NMR spectroscopy and by molecular simulations. The preferred conformations of compound **1** in DMSO-d_6 and in water (pH 3.5) (Fig. 4) were derived from experimental data (NOEs, $^3J_{\alpha H\text{-}NH}$ coupling constants, temperature coefficients of amide protons) through distance geometry calculations and restrained molecular dynamics simulations as described in Tables 2–5. The results suggest that compound **1** exhibits similar backbone conformations in both solvents with a type II′ β-turn about Phe^3-(D)-Trp^4-Lys^5-Thr^6 which is further stabilized by the hydrogen bond between NH(Thr^6) and C=O(Phe^3). The type II′ β-turn is confirmed by the strong $d_{\alpha N}(4,5)$ NOE, the medium $d_{NN}(5,6)$ NOE (Table 2) and the low temperature coefficient of the amide proton of Thr^6 in DMSO-d_6 (Table 5). The rest of the peptidic backbone exhibits an extended conformation as suggested by the strong sequential $d_{\alpha N}(2,3)$, $d_{\alpha N}(3,4)$ and $d_{\alpha N}(6,7)$ NOEs (Table 2) and the

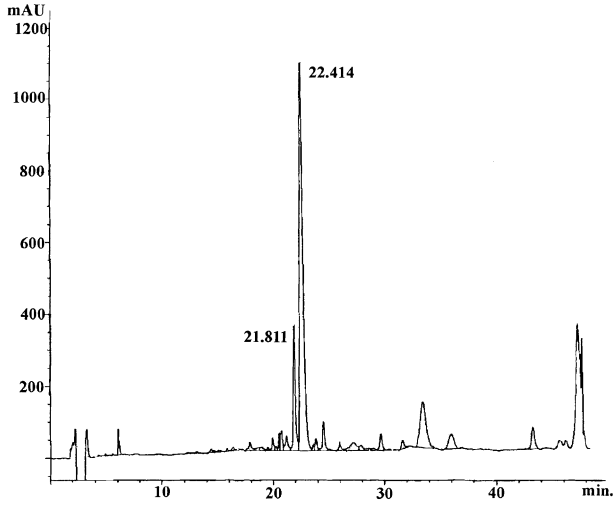

Figure 2. HPLC profile after peptide cleavage indicating the 5:1 ratio of the compound **1** to its epimer **2** (Compound **1**: R_t 22.414 min.; compound **2**: R_t 21.811 min.)

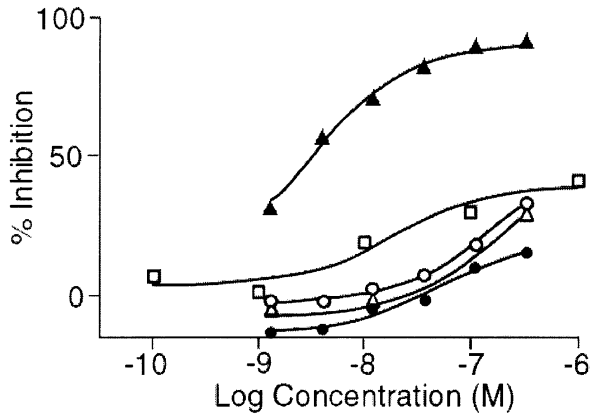

Figure 3. Binding of compound **1** (PTR-3205) to membranes isolated from cells expressing cloned human somatostatin receptors: hsstr1●; hsstr2▲; hsstr3○; hsstr4□; hsstr5△.

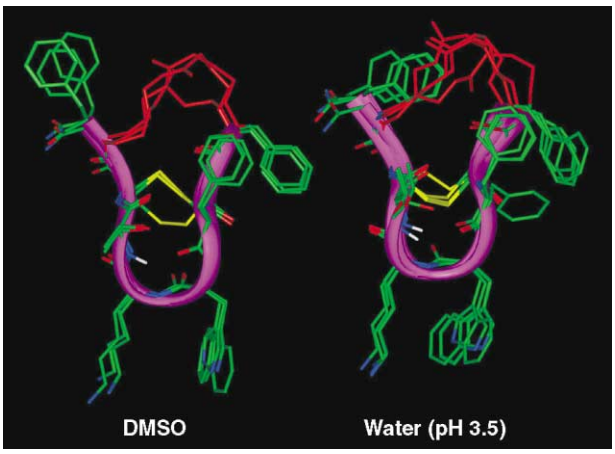

Figure 4. Front view of the preferred conformational cluster for compound **1** in DMSO-d_6 (left) and in water (right). Disulfide bridge in yellow; lactam bridge in red.

Table 1. Optical purity of the amino acid residues in compounds **1** and **2**

Amino acid	% in **1**	% in **2**
D-Threonine	<0.1	<0.1
L-Threonine	99.7	>99.3
D-allo-Threonine	0.1	<0.6
L-allo-Threonine	<0.1	<0.1
L-Cysteine	<0.1	43.1
	D-Enantiomer	D-Enantiomer
L-Phenylalanine	<0.1	<0.1
	D-Enantiomer	D-Enantiomer
L-Lysine	<0.1	<0.1
	D-Enantiomer	D-Enantiomer
D-Tryptophan	<3.2	<2.3
	L-Enantiomer	L-Enantiomer

Table 2. Summary of the observed backbone NOEs of compound **1** in water and in DMSO-d_6. NOEs are classified as strong (s), medium (m) or weak (w)

NOE	Water	DMSO-d_6
$\alpha H^1 \sim NH^2$	s	s
$\alpha H^2 \sim NH^2$	m	m
$\alpha H^2 \sim NH^3$	s	s
$\alpha H^3 \sim NH^3$	[a]	s
$\alpha H^3 \sim NH^4$	s	s
$\alpha H^4 \sim NH^4$	m	m
$\alpha H^4 \sim NH^5$	s	s
$\alpha H^5 \sim NH^5$	m	m
$\alpha H^5 \sim NH^6$	m	m
$NH^5 \sim NH^6$	m	m
$\alpha H^6 \sim NH^6$	m	m
$\alpha H^6 \sim NH^7$	s	s
$\alpha H^7 \sim NH^7$	[a]	m
$\alpha H^2 \sim \alpha H^7$	m	m
$NH^6 \sim NH^7$	[a]	m–w
$\alpha H^5 \sim NH^7$	m–w	[a]
$\alpha H^7 \sim H_{41}$	m–w	m–w
$\alpha H^7 \sim H_{42}$	s	m–s
$\alpha H^7 \sim H_{51}$	m	m
$\alpha H^7 \sim H_{52}$	m	m
$\alpha H^8 \sim H_{51}$	m–s	m

[a]No signal observed due to presaturation.

Table 3. Summary of the observed side chain NOEs of compound **1** in water and in DMSO-d_6. NOEs are classified as strong (s), medium (m) or weak (w)

Residue	Water	DMSO-d_6
Phe^3		
$\alpha H \sim \beta H_1$	m–s	m–s
$\alpha H \sim \beta H_2$	s	m–s
$NH \sim \beta H_1$	m–w	m
$NH \sim \beta H_2$	[a]	[a]
(D)Trp^4		
$\alpha H \sim \beta H_1$	s	s
$\alpha H \sim \beta H_2$	w	w
$NH \sim \beta H_1$	m–s	s
$NH \sim \beta H_2$	s	s
Lys^5		
$\alpha H \sim \beta H_1$	w	w
$\alpha H \sim \beta H_2$	s	m–s
$NH \sim \beta H_1$	s	m–s
$NH \sim \beta H_2$	m–w	[a]

[a]No signal observed due to presaturation.

large $^3J_{\alpha H\text{-}NH}$ coupling constants (Table 4). High temperature coefficients measured for the Cys^2, (D)-Trp^4 and Cys^7 amide protons (−5.0, −4.5 and −4.2 ppb/K, respectively) and the low temperature coefficient for the Phe^3 amide proton (−2.1 ppb/K) are fully consistent with the extent of solvent exposure expected for these protons in the antiparallel β-sheet-like structure. Figure 4 shows the front view of the preferred conformational cluster of compound **1** in which the backbone assumes the antiparallel β-sheet-like conformation.

The medium NOE between the αH of Lys^5 and the amide proton of Cys^7 in water (Fig. 5) suggests a 'folded' antiparallel β-sheet-like structure as seen from the side view of compound **1** (Fig. 6). To our knowledge, this is the first direct evidence observed for this conformation. Based on a series of active somatostatin analogues, we have previously proposed a 'folded,' rather than a 'flat' β-sheet as the bioactive conformation.[15–17] For sandostatin, X-ray data,[9] NMR data and molecular dynamics simulations[8] suggest that the molecule in solution exists in an equilibrium between a β-sheet and a partially helical structure,

Table 4. The $^{3}J_{\alpha H\text{-}NH}$ coupling constants and the calculated dihedral angles of compound **1** in water and in DMSO-d_6

Residue	Water		DMSO-d_6	
	$J_{\alpha H\text{-}NH}$ (Hz)[a]	ϕ (deg)[b]	$J_{\alpha H\text{-}NH}$ (Hz)[a]	ϕ (deg)[b]
Cys[2]	7.5	45, 75, −88, −152	8.6	−97, −143
Phe[3]	8.5	−96, −144	8.0	60, −92, −148
(D)Trp[4]	5.2	74, 166, −24, −96	6.8	84, 156, −37, −83
Lys[5]	8.9	140, −100	8.2	−94, −146
Thr[6]	8.8	141, −99	9.0	−101, −139
Cys[7]	7.1	40, 79, −86, −154	8.5	−96, −144

[a] $^{3}J_{\alpha H\text{-}NH}$ values are within 0.5 Hz.
[b] ϕ values were calculated according to $J = A\cos^2|\phi \pm 60°| + B\cos|\phi \pm 60°| + C$ where (+) is for D-configuration residues and (−) for L-configuration residues, (A, B, C) = (8.6, 1.0, 0.4) as proposed by Bystrov[18] for a chiral residue.

Table 5. Temperature coefficients of amide protons of compound **1** in DMSO-d_6

Residue	Phe[1]	Cys[2]	Phe[3]	Trp[4]	Lys[5]	Thr[6]	Cys[7]
-ppb/K	2.8	5.0	2.1	4.5	4.3	1.2	4.2

where the residues at the end of the backbone 'curl' above the plane of the β-turn and the disulfide bridge, and into a 3_{10} helix-like array. Morgan[17] defined this conformational array as the 'helix-turn-sheet' (H-T-S) motif.

The hexapeptide Cys[2]-Phe[3]-(D)-Trp[4]-Lys[5]-Thr[6]-Cys[7] is cyclized by a disulfide bond and is further constrained by the hydrogen bond between NH(Thr[6]) and C=O(Phe[3]). This backbone part of the molecule is rigid and consequently, determines much of the overall conformation of the compound. The second ring composed of the *N*-alkylated Phe[1] and Phe[8] residues, is more flexible due to the presence of the additional methylene units. Molecular simulations suggest that the peptide bond between Cys[7] and Phe[8] adopts a *trans* conformation. The nitrogen atom of Phe[1] is protonated, both in water (pH 3.5) and in DMSO-d_6. In DMSO-d_6, the 1-D spectrum indicated two broad signals at 9.26 and 9.05 ppm (Table 6), and the TOCSY showed two parallel sets of AMX spin systems in the fingerprint region. The *trans* conformation of the lactam bond, the protonation of the Phe[1] amine and the flexibility of the lactam bridge do not allow the lactam and the disulfide bridge to orient on the same side as the β-sheet formed by the backbone. RMD simulations gave rise to two main orientations of the lactam bridge with respect to the backbone: extended (Fig. 7, left) or bent (Fig. 7, right).

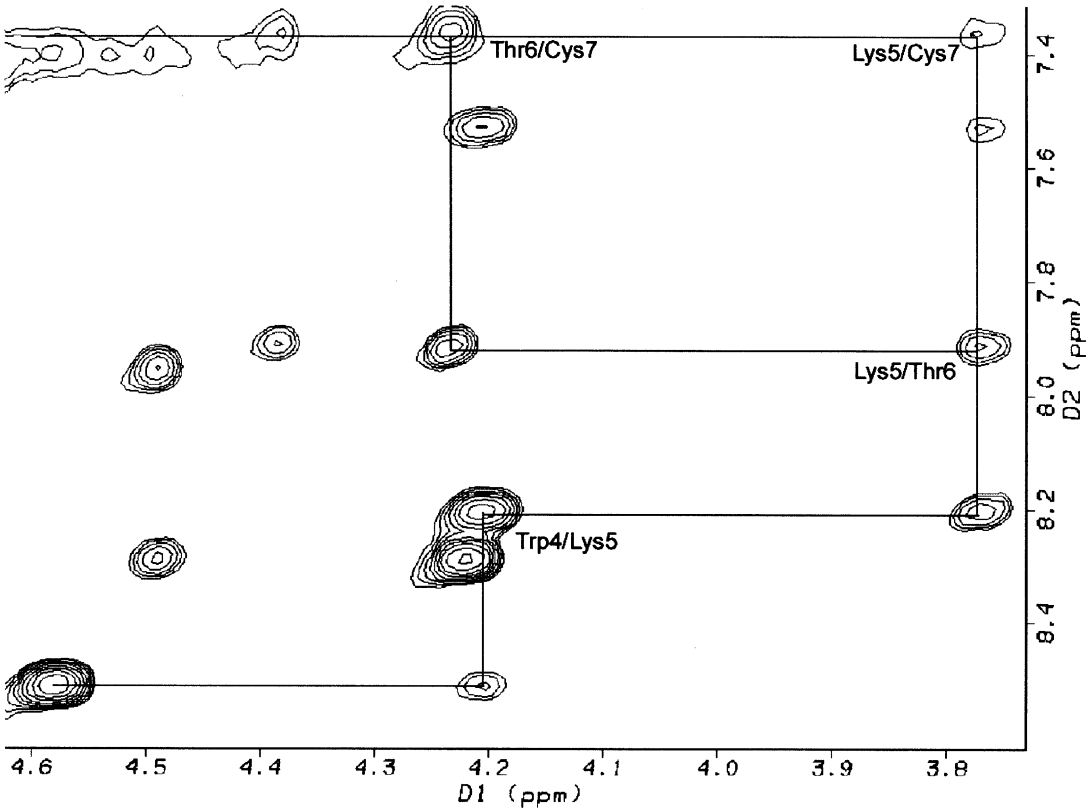

Figure 5. Fingerprint region of 2-D ROESY (200 ms) spectrum for compound **1** in water (pH 3.5).

Only the extended structure was consistent with all NOE restraints. Thus, we propose that the preferred conformation of compound **1** is a 'folded' β-sheet-like structure, with the lactam bridge extending out in the plane of the β-turn. This structure can be then categorized as an 'S-T-S' motif (sheet-turn-sheet), as described by Morgan.[17] It has been shown that somatostatin analogues selective at hsst2 exhibit a 'S-T-S' motif which is in agreement with our experimental findings.[17] In addition, Figure 8 shows the front (left) and the rear (right) views of the preferred structures from 1 ns of molecular dynamics simulations. It is readily seen from these views that the disulfide and lactam bridges enhance the preferences for the type II′ β-turn about the (D)-Trp-Lys dipeptide residues.

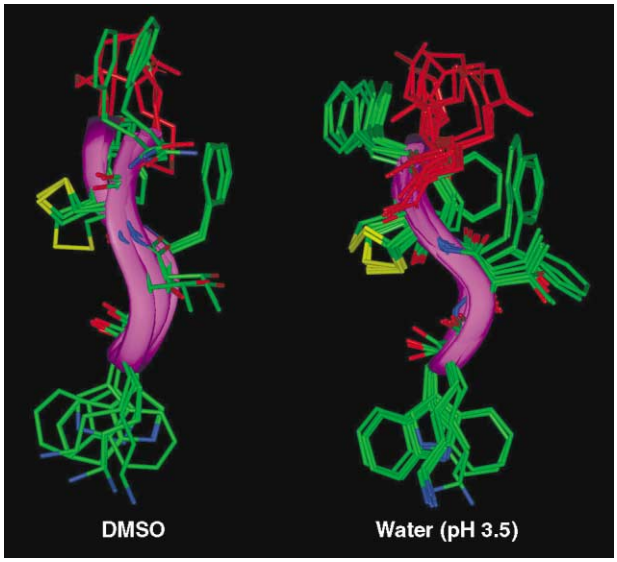

Figure 6. Side view of the preferred conformational cluster for compound **1** in DMSO-d_6 (left) and in water (right). Disulfide bridge in yellow; lactam bridge in red.

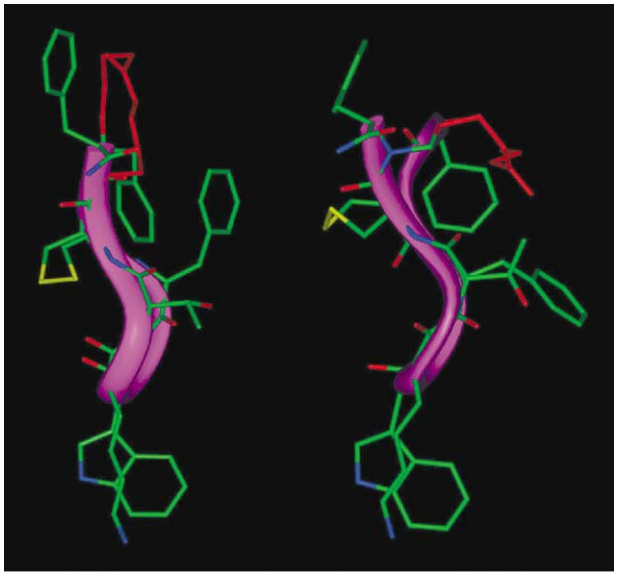

Figure 7. Extended (left) and bent (right) orientations of the lactam bridge (red) with respect to the backbone in compound **1**.

Side chain conformations

As with all other bioactive somatostatin analogues, the predominant side chain orientations of (D)-Trp[4] and Lys[5] are *trans (t)* and *gauche (g⁻)*, respectively. This orientation was confirmed by the $^3J_{\alpha H\text{-}NH}$ coupling constants (Table 7) and the NOE intensities between the NH∼βH and αH∼βH of these residues (Table 3). The relatively high field chemical shift value for the γH of Lys[5] (Table 6) arises from the shielding effects of the aromatic ring of (D)-Trp[4] as previously reported[9] and supports the respective *trans* and *gauche* orientations. As a result, the side chains of these residues are closely aligned. As expected and observed in the 1 ns MD simulation at 300 K (Fig. 8), the side chains of (D)-Trp[4] and Lys[5] are flexible compared to the relative rigidity of the backbone which, as noted above, is constrained by the coexistence of the type II′ β-turn, disulfide and lactam bridges.

Table 6. Chemical shifts of compound **1** in water and in DMSO-d_6

Residue	Proton	Water (ppm)	DMSO-d_6 (ppm)
Phe[1]	NH	—	9.05/9.26
	α	4.22	4.390
	β	3.24/3.40	3.02
Cys[2]	NH	8.28	8.73
	α	4.49	4.68
	β	2.76/3.02	2.86/3.11
Phe[3]	NH	7.95	7.76
	α	4.58	4.68
	β	2.83/2.97	2.76/2.87
(D)Trp[4]	NH	8.51	8.76
	α	4.20	4.16
	β	2.73/2.93	2.76/2.92
Lys[5]	NH	8.21	8.58
	α	3.77	3.79
	β	1.25/1.53	1.40/1.70
	γ	0.35/0.54	0.80
	δ	1.23/1.31	1.34
Thr[6]	NH	7.91	7.82
	α	4.24	4.22

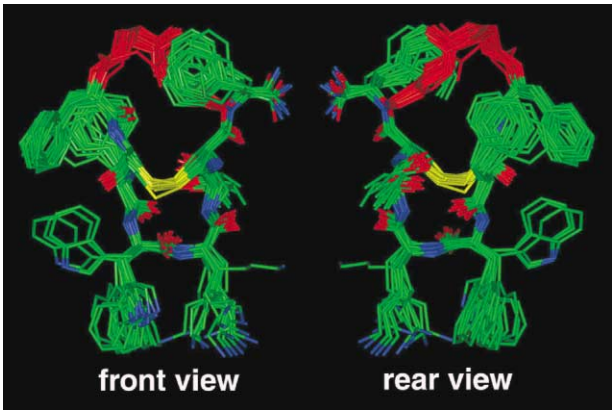

Figure 8. Trajectories from the 1 ns restrained molecular dynamics simulations of compound **1** at 300 K. The front view shows the disulfide bridge (yellow) toward the viewer and the lactam bridge (red) away from the viewer; whereas, the rear view shows the disulfide bridge (yellow) away from the viewer and the lactam bridge (red) toward the viewer. With both views, it is possible to obtain a complete picture of the conformational relationship of the disulfide and lactam bridges.

Conclusions

We have designed and synthesized an hsst2 selective analogue of somatostatin. The selectivity of compound **1** towards hsst2 was determined in vitro, by binding assays to the five cloned individually expressed receptors. We also studied the conformation of this compound in water and in DMSO-d_6. We found that this compound adopts a 'folded' β-sheet-like structure in opposite orientation to the disulfide bridge, with the lactam bridge extending in approximately the same plane as the type II' β-turn. We propose that this array limits the number of conformational minima available to the molecule as a whole. The pharmacophoric region Phe^3-(D)-Trp^4-Lys^5-Thr^6 of compound **1** overlaps well with those of the Veber compound L-363,301 c[Pro-Phe-(D)-Trp-Lys-Thr-Phe], sandostatin (D)-Phe-c[Cys-Phe-(D)-Trp-Lys-Thr-Cys]-Thr-ol and a lanthionine-

Table 7. The $^3J_{\alpha H\text{-}\beta H}$ coupling constants and the calculated side chains populations of compound **1** in water and DMSO-d_6

	Water		DMSO-d_6	
Residue	$J_{\alpha H\text{-}\beta H}$[a]	t, g$^-$, g$^+$[b]	$J_{\alpha H\text{-}\beta H}$[a]	t, g$^-$, g$^+$[b]
Phe^3	6.0/6.7	0.24, 0.36, 0.40	6.7/7.2	0.30, 0.36, 0.34
(D)-Trp^4	9.0/6.3	0.53, 0.22, 0.25	8.7/6.0	0.51, 0.20, 0.29
Lys^5	10.2/3.9	0.12,0.70, 0.18	9.5/4.3	0.16, 0.63, 0.21
Thr^6	3.6	0.10(g$^-$)	3.7	0.10(g$^-$)

[a]$^3J_{\alpha H\text{-}\beta H}$ coupling constants were analyzed using the three state rotamer approximation.
[b]The side chain populations were calculated using $J_T = 13.56$ Hz and $J_G = 2.60$ Hz for nonaromatic residues and $J_T = 13.85$ Hz and $J_G = 3.55$ Hz for aromatic residues.[18]

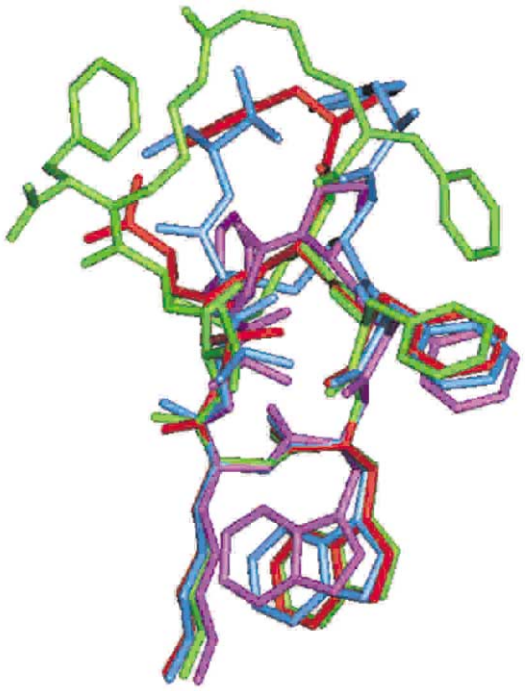

Figure 9. Overlap of the preferred structure of compound **1** with the preferred conformations of three well studied somatostatin analogues that bind with high affinities to hsstr2 and hsstr5 and with moderate affinity to hsstr3 [compound **1** (green); Veber compound L-363,301 (Merck)(purple); sandostatin (blue); lanthionine-heptamer (red)-all illustrated in Figure 10].

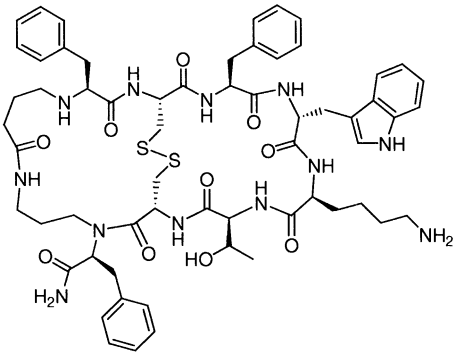

compound **1** (green)

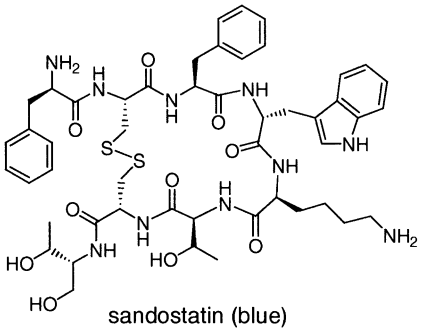

sandostatin (blue)

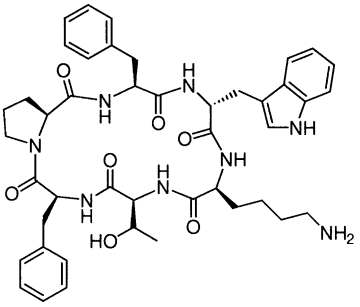

Veber compound L-363,301 (Merck) (purple)

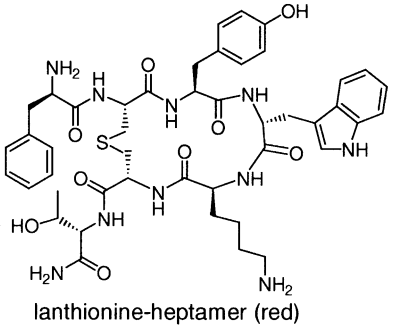

lanthionine-heptamer (red)

Figure 10. Compound 1 (green), Veber compound L-363, 301(purple), sandostatin (blue) and the lanthionine-heptamer (red).

heptameric compound (D)-Phe-c[Ala_L-Tyr-(D)-Trp-Lys-Ala_L]-Thr-NH_2 which are all hsst2 selective with a somewhat reduced potency at hsst5 (Figs 9 and 10). These features are in agreement with previously established structural elements of hsst2 and hsst5 selective molecules. As seen in Figure 9, the lactam bridge and the two exocyclic hydrophobic residues at positions 1 and 8 of compound **1** occupy a larger volume than the equivalent region of the other molecules. This could hinder its ability to bind to the hsst5 receptor, leading to the observed selectivity.

Experimental

Synthesis of compound 1 (PTR-3205)

In a reaction vessel equipped with a sintered glass bottom, Rink Amide MBHA resin, NOVA (subst. level 0.46 mmol/g, 2 g) was swelled in NMP by agitation overnight. The Fmoc group was removed from the resin upon treatment with 25% piperidine in NMP (2×16 mL). After washing the resin with NMP (7×10–15 mL), Fmoc-PheN3(Alloc)-OH (3 equiv, 2.76 mmol, 1.46 g) dissolved in NMP (16 mL) was activated with PyBroP (3 equiv, 2.76 mmol, 1.28 g) and DIEA (6 equiv, 5.52 mmol, 0.95 mL) for 4 min at room temperature (rt), transferred to the reaction vessel and allowed to react for 1 h at rt. Following coupling, the peptidyl-resin was washed with NMP (7×10–15 mL). Completion of reaction was monitored by the ninhydrin test (Kaiser test). The removal of Fmoc and NMP washes were carried out as described above followed by THF washes (3×10–15 mL). Fmoc-Cys(Acm)-OH (5 equiv, 4.6 mmol, 1.9 g) was then double coupled, each time using BTC (1.65 equiv, 1.52 mmol, 0.45 g) and a 0.14 M solution of collidine (14 equiv, 12.88 mmol, 1.7 mL) in THF (30–35 mL) at 50 °C for 1 h. Sequential amino acid coupling of Fmoc-Thr(tBu)-OH, Fmoc-Lys(Boc)-OH, Fmoc-(D)-Trp(Boc)-OH, Fmoc-Phe-OH, Fmoc-Cys(Acm)-OH and Fmoc-PheC3(O-Allyl)-OH was accomplished as previously described. After the last amino acid coupling, the peptidyl-resin was washed with DCM (3×10–15 mL,) and 92.5:5:2.5 DCM/AcOH/NMM (3×10–15 mL). In order to remove the allyl and Alloc groups, a yellow suspension of $Pd(PPh_3)_4$ (2.6 mmol, 3.0 g) in the DCM/AcOH/NMM solution (80 mL) was transferred to the reaction vessel, followed by degassing with Ar and vigorous agitation for 2 h in the dark. The peptidyl-resin was washed with DCM, $CHCl_3$ and NMP (each 5×10–15 mL). On-resin peptide cyclization to form the lactam bridge was accomplished using PyBOP (3 equiv, 2.76 mmol, 1.44 g) and DIEA (6 equiv, 5.52 mmol, 0.95 mL) in NMP (20 mL) at rt for 1 h and then repeated overnight under the same conditions. The peptidyl-resin was washed with NMP and 4:1 DMF/water (3×15 mL). A solution of I_2 (10 equiv, 9.2 mmol, 2.32 g) in 4:1 DMF/water (23 mL) was added to the peptidyl-resin followed by agitation at rt for 40 min to afford the disulfide bridge cyclization. The peptidyl-resin was filtered and washed extensively with 4:1 DMF/water, DMF, NMP, DCM, $CHCl_3$ and 2% ascorbic acid in DMF. After the final Fmoc deprotection and subsequent washings as described above, the peptidyl resin was washed with MeOH and dried under vacuum for 20 min. The peptide was cleaved from the resin using a cocktail solution of 95:2.5:2.5 TFA/TIS/H_2O (30 mL) for 30 min at 0 °C under Ar atmosphere and then for 1.5 h at rt. The resin was filtered and washed with the cocktail solution (4–5 mL) and TFA (4–5 mL), and the filtrate solution was evaporated by a stream of N_2 to give an oily residue. Upon the addition of cold Et_2O, the oily residue solidified. Centrifugation and decantation of the Et_2O layer and repeated treatment with additional cold Et_2O afforded the crude white solid **1** which was purified by RP-HPLC (0.388 g, 30%). $C_{16}H_{79}N_{12}O_{10}S_2$; MS (MALDI-FTMS) $m/z = 1203.55$ ($M+H$), 1225.53 ($M+Na^+$), calcd; 1225.5254 ($M+Na^+$), found.

Purification of compound 1 (PTR-3205)

Preparative RP-HPLC purification and analysis was carried out on a Waters Delta Prep 4000 preparative high pressure liquid chromatography system (Waters 486 UV–vis tunable absorbance detector and Waters fraction collector, controlled by the Millennium v3.05 program). The flow rate was set to 15 mL/min, using a preparative column (Vydac C-18, 218TP101550, 50×250 mm, 10–15 μ), and the detector was set at a wavelength of 214 nm and the fraction collector, at a time mode of 10 s/fraction. Solvents used in HPLC purification were as follows: solvent A: 0.1% TFA/H_2O; solvent B: 0.1% TFA/CH_3CN.

Analytical RP-HPLC of the peptide sample was performed by a Waters 2690 Separation module equipped with a Waters 996 Photodiode Array Detector. The column (Vydac C-18, 218TP54, 4.6×250 mm, 5 μ) flow rate was set at 1 mL/min and the detector wavelength was set at 214 nm. The purified peptide eluted with a retention time of 19.78 min from 90% A:10% B to 10% A:90%B over 30 min.

Radioligand binding assays

Radioligand binding assays were carried out on membranes prepared from CHO-K1 cells which are stable for expressing individually cloned somatostatin receptors. Cells were grown for 2 days to almost confluency and washed and scraped into Buffer A (50 mM ice-cold Tris–HCl solution, pH 7.8, containing 1 mM EGTA, 5 mM $MgCl_2$, 10 μg/mL leupeptin, 200 μg/mL bacitracin, 0.1 mM PMSF, and 0.5 μg/mL aprotinin). The suspension was centrifuged at 10,000 rpm for 10 min at 4 °C (in Sorvall RC 26 Plus ultracentrifuge, rotor SS-34). The pellet was resuspended in Buffer A and homogenized with a Polytron PT 1200 homogenizer (Kinematica AG, Switzerland) for 10 s (setting 2, 3 strokes). The homogenate was then centrifuged at 20,000 rpm for 20 min at 4 °C. The pellet was resuspended in Buffer A and homogenized using the Polytron homogenizer for 5 s (setting 2, 3 strokes). The protein content was determined by Bradford test, and the membrane preparation was diluted in Buffer A containing 1 mg/mL BSA to a final concentration of 0.2 or 0.4 mg/mL membrane

protein (depending on the specific somatostatin receptor used).

The radioligand binding assay was performed in a 96-well microtiter plate (Maxisorp plates, Nunc, Denmark). Cell membranes (10 or 20 μg protein) were incubated with ^{125}I-Tyr^{11} somatostatin-14 (0.05 μCi; specific activity 2000 Ci/mmol) in a final volume of 250 μL, for 45 min at rt, in the presence or absence of competing peptides. Nonspecific binding was defined as the radioactivity remaining bound in the presence of 1 μM somatostatin. At the end of the binding reaction, free radioligand was separated from bound ligand by rapid filtration through UniFilter GF/C plates preincubated in a solution of 5 g/L polyethylenimine and 1 g/L BSA. The filtration was performed in a FilterMate Cell Harvester (Packard Instrument Company, USA). After filtration, the filters were washed several times with 50 mM Tris–HCl pH 7.8 and allowed to dry overnight at rt, afterwards which 50 μL scintillation liquid was added to each filter and bound radioactivity was counted by TopCount Microplate Scintillation Counter (Packard). Data from radioligand binding were used to generate inhibition curves, and IC_{50} values were determined for each of the tested peptides.

NMR spectroscopy

The NMR experiments were carried out in DMSO-d_6, H_2O and D_2O. The samples were prepared by dissolving compound **1** in 0.5 mL 9:1 H_2O/D_2O. The pH value of the sample was adjusted to 3.5 ± 0.05 by the addition of small aliquots of 0.1 M HCl or NaOH. After lyophilization, the sample was dissolved in 0.5 mL D_2O (99.96%) in order to give the deuterated sample for analysis.

All NMR experiments were carried out on a 500 MHz Bruker AMX500 spectrometer at 300 K. 1-D spectra were acquired between 300 and 320 K to measure the temperature coefficients of the amide protons. All 2-D NMR spectra were recorded in phase-sensitive mode using time proportional phase increment (TPPI) and quadrature detection in both dimensions. Double quantum filtered COSY (DQF-COSY) spectra were acquired with the pulse sequence reported by Derome et al.[19] TOCSY spectra were obtained using the MELV-17 spin lock sequence[20] with mixing times of 35 ms and 70 ms. When necessary, TOCSY spectra with a mixing time of 50 ms were acquired at 320 K to obtain the temperature coefficients of the amide protons. ROESY and NOESY spectra were acquired by using the method of States et al.[21] where the reported mixing times were 100, 200 and 300 ms. Suppression of the water resonance was accomplished by a presaturation method through continuous irradiation during the relaxation delay (1.5 s). All spectra were collected with 2048 data points in w2 and 512 t1 increments and zero-filled to 2048×1024 data points during the data processing. The DQF-COSY experiments were obtained using 4096×512 data points and processed with 4096×1024 data points. Chemical shifts were referenced to DMSO-d_6 (2.49 ppm) and H_2O (4.75 ppm) for experiments in DMSO-d_6 and water, respectively. The coupling constants were obtained by 1-D ^{1}H NMR and 2-D DQF-COSY spectra and the NOE cross peak volumes were calibrated against the distance between the two β-protons of the Lys^5 on the basis of ISPA (isolated spin pair approximation). The restraints were classified as strong, medium and weak with distance upper limits of 2.5, 3.5 and 4.5 Å respectively.

Molecular modeling

The computational protocol for structural determination in solution consisted of a distance geometry (DG) conformational search, restrained molecular dynamics (RMD) simulations, energy minimization and cluster analysis. The distance geometry program DGII was used to generate structures consistent with the distance restraints derived from the NOE intensities. The ϕ torsion angles and hydrogen bonding pattern of the DGII structures were compared with the values derived from the NMR data. A Karplus-type equation[22] was used to compute the ϕ torsion angles consistent with the measured $^3J_{\alpha H \sim NH}$ coupling constants, while allowing a tolerance of $\pm 30^\circ$. In the case of hydrogen bond based selection, structures were retained in which amide protons with a temperature coefficient less than -2 ppb/K donate at least one hydrogen bond in DMSO-d_6.[23] Structures, which were not consistent with the experimentally derived torsional angles, temperature coefficients or distance restraints were discarded. The remaining structures were subjected to a restrained dynamics simulation.

Restrained molecular dynamics simulations were carried out in vacuo employing the DISCOVER (v97.2) program[24] with the CFF91 force field. The NOE restraints were included with a force constant of 25 kcal/(mol Å^2). A distance dependent dielectric constant was used to take into account the solvent effect.[25] A charged form of the amino group in the Lys^5 side chain was used in order to be consistent with the actual situation under physiological condition. No cross terms or Morse terms were used during the simulation and all normal peptide bonds were kept in their *trans* configuration.

Prior to every restrained molecular dynamics simulation, the system was equilibrated for 3 ps. After that period, the selected DGII structures were submitted to molecular dynamics of 10 ps at 1000 K with a step size of 1 fs. At regular intervals of 1 ps, conformations were extracted and subjected to a preliminary energy minimization by the steepest descent method until the maximum derivative was less than 1 kcal/mol. Starting from each of these minimized structures, an additional molecular dynamics analysis of 10 ps was carried out at 300 K. Again, at regular intervals of 1 ps, unrestrained minimization was performed to generate ensembles of minimized structures with the VA09A algorithm so that the maximum derivative was less than 0.01 kcal/mol. The molecular dynamics simulation led to 100 minimized structures for each structure selected from DGII calculation. The resulting conformations were then

examined and selected according to their consistency with the NOEs, $^3J_{NH\text{-}\alpha H}$ coupling constants and hydrogen bonding data. Those structures consistent with the experimental results and with energies not higher than 10 kcal/mol above the lowest energy conformation were selected for cluster analysis to obtain the predominant molecular conformations in solution.[26,27]

Acknowledgements

We wish to thank the National Institutes of Health (DK15410) for their financial support. The purification of compounds **1** and **2** was performed by Manuela Lazarov and Dvira Shohat from Peptor's analytical group. We gratefully acknowledge their invaluable help. We acknowledge Juliann Kwak for her critical reading of the manuscript and Nicole Smith for her help in preparing the figures, as well as Sandra Blaj Moore for the Introduction, revision and preparation of the manuscript for submission.

References and Notes

1. (a) Brazeau, P.; Vale, W.; Burgus, R.; Ling, N.; Butcher, M.; Rivier, J.; Guillemin, R. *Science* **1973**, *179*, 77. (b) Burgus, R.; Ling, N.; Butcher, M.; Guillemin, R. *Proc. Natl. Acad. Sci. U.S.A.* **1973**, *70*, 684.
2. Gerich, J. E.; Lovinger, R.; Grodsky, G. M. *Endocrinology* **1975**, *96*, 749.
3. (a) Tamminga, C. A.; Foster, N. L.; Fedio, P.; Bird, E. D.; Chase, T. N. *Neurology* **1987**, *37*, 161. (b) Schettini, G.; Florio, T.; Magri, G.; Grimaldi, M.; Meucci, O.; Landolfi, E.; Marino, A. *Eur. J. Pharmacol.* **1988**, *151*, 399. (c) DeNoble, V. J.; Hepler, D. J.; Barto, R. A. *Brain Res.* **1989**, *482*, 42.
4. Patel, Y. C. *Frontiers in Neuroendocrinology* **1999**, *20*, 157.
5. (a) Veber, D. F.; Freidlinger, R. M.; Perlow, D. S.; Paleveda, W. J., Jr.; Holly, F. W.; Strachan, R. G.; Nutt, R. F.; Arison, B. H.; Homnick, C.; Randall, W. C.; Glitzer, M. S.; Saperstein, R.; Hirschmann, R. *Nature* **1981**, *292*, 55. (b) Arison, B. H.; Hirschmann, R.; Veber, D. F. *Bioorg. Chem.* **1978**, *7*, 447. (c) Veber, D.F. In *Peptides: Proceedings of the Sixth American Peptide Symposium*; Gross, E., Meyenhofer, J., Eds.; Pierce Chemical Company: Rockford, IL, 1995, pp 409
6. Hocart, S. J.; Jain, R.; Murphy, W. A.; Taylor, J. E.; Morgan, B.; Coy, D. H. *J. Med. Chem.* **1998**, *41*, 1146.
7. Bauer, W.; Briner, U.; Doepfner, W.; Haller, R.; Huguenin, R.; Marbach, P.; Petcher, T. J.; Pless, J. *Life Sci.* **1982**, *31*, 1133.
8. Melacini, G.; Zhu, Q.; Goodman, M. *Biochemistry* **1997**, *36*, 1233.
9. Pohl, E.; Heine, A.; Sheldrick, G. M.; Dauter, Z.; Wilson, K. S.; Kallen, J.; Huber, W.; Pfaffli, P. J. *Acta Crystallogr., Sect. D-Bio. Cryst* **1995**, *51*, 48.
10. Gilon, C.; Huenges, M.; Matha, B.; Gellerman, G.; Hornik, V.; Afargan, M.; Amitay, O.; Ziv, O.; Feller, E.; Gamliel, A.; Shohat, D.; Wanger, M.; Arad, O.; Kessler, H. *J. Med. Chem.* **1998**, *41*, 919.
11. Insight II: Search Compare, Molecular Simulations Inc., 1995.
12. Cai, R. Z.; Szoke, B.; Lu, R.; Fu, D.; Redding, T. W.; Schally, A. V. *Proc. Nat. Acad. Sci. U.S.A.* **1986**, *83*, 1896.
13. Falb, E.; Yechezkel, T.; Salitra, Y.; Gilon, C. *J. Pept. Res.* **1999**, *53*, 507.
14. Kamber, B.; Hartmann, A.; Eisler, K.; Riniker, B.; Rink, H.; Sieber, P.; Rittel, W. *Helv. Chim. Acta* **1980**, *63*, 899.
15. Huang, Z. W.; He, Y. B.; Raynor, K.; Tallent, M.; Reisine, T.; Goodman, M. *J. Am. Chem. Soc.* **1992**, *114*, 9390.
16. Mattern, R. H.; Zhang, L.; Rueter, J. K.; Goodman, M. *Biopolymers* **2000**, *53*, 506.
17. Morgan, B. In *XVIII Corso Avanzato in Chimica Farmaceutica e Seminario Nazionale per Dottorandi 'E. Duranti*, Urbino, Italy, June 29–July 3rd, 1998.
18. Bystrov, V. F.; Ivanov, V. T.; Portnova, S. L.; Balashova, T. A.; Ovchinnikov, Yu. A. *Tetrahedron* **1973**, *29*, 873.
19. Derome, A. E.; Williamson, M. P. *J. Magn. Reson.* **1990**, *88*, 177.
20. Bax, A. D.; Davis, D. G. *J. Magn. Reson.* **1985**, *65*, 355.
21. States, D. J.; Haberkorn, R. A.; Ruben, D. J. *J. Magn. Reson.* **1982**, *48*, 286.
22. Karplus, M. *J. Am. Chem. Soc.* **1963**, *85*, 2870.
23. Kessler, H. *Angew. Chem.* **1982**, *94*, 509.
24. Hagler, A. T., In *The Peptides*, Udenfriend, S., Meienhofer, J., Eds. Academic: Orlando, 1985; Vol. 7, p 213.
25. Leach, A. R. *Molecular Modeling: Principles and Applications*; Longman: New York, 1996.
26. Kazmierski, W. M.; Ferguson, R. D.; Lipkowski, A. W.; Hruby, V. J. *Int. J. Pept. Protein Res.* **1995**, *46*, 265.
27. Yamazaki, T.; Mierke, D. F.; Said-Nejad, O. E.; Felder, E. R.; Goodman, M. *Int. J. Pept Protein Res.* **1992**, *39*, 161.